



The High Power Electric Propulsion (HiPEP) Ion Thruster

John E. Foster, Tom Haag, and Michael Patterson
Glenn Research Center, Cleveland, Ohio

George J. Williams, Jr.
Ohio Aerospace Institute, Brook Park, Ohio

James S. Sovey
Alpha-Port, Inc., Cleveland, Ohio

Christian Carpenter
QSS Group, Inc., Cleveland, Ohio

Hani Kamhawi, Shane Malone, and Fred Elliot
Glenn Research Center, Cleveland, Ohio

The NASA STI Program Office . . . in Profile

Since its founding, NASA has been dedicated to the advancement of aeronautics and space science. The NASA Scientific and Technical Information (STI) Program Office plays a key part in helping NASA maintain this important role.

The NASA STI Program Office is operated by Langley Research Center, the Lead Center for NASA's scientific and technical information. The NASA STI Program Office provides access to the NASA STI Database, the largest collection of aeronautical and space science STI in the world. The Program Office is also NASA's institutional mechanism for disseminating the results of its research and development activities. These results are published by NASA in the NASA STI Report Series, which includes the following report types:

- **TECHNICAL PUBLICATION.** Reports of completed research or a major significant phase of research that present the results of NASA programs and include extensive data or theoretical analysis. Includes compilations of significant scientific and technical data and information deemed to be of continuing reference value. NASA's counterpart of peer-reviewed formal professional papers but has less stringent limitations on manuscript length and extent of graphic presentations.
- **TECHNICAL MEMORANDUM.** Scientific and technical findings that are preliminary or of specialized interest, e.g., quick release reports, working papers, and bibliographies that contain minimal annotation. Does not contain extensive analysis.
- **CONTRACTOR REPORT.** Scientific and technical findings by NASA-sponsored contractors and grantees.

- **CONFERENCE PUBLICATION.** Collected papers from scientific and technical conferences, symposia, seminars, or other meetings sponsored or cosponsored by NASA.
- **SPECIAL PUBLICATION.** Scientific, technical, or historical information from NASA programs, projects, and missions, often concerned with subjects having substantial public interest.
- **TECHNICAL TRANSLATION.** English-language translations of foreign scientific and technical material pertinent to NASA's mission.

Specialized services that complement the STI Program Office's diverse offerings include creating custom thesauri, building customized databases, organizing and publishing research results . . . even providing videos.

For more information about the NASA STI Program Office, see the following:

- Access the NASA STI Program Home Page at <http://www.sti.nasa.gov>
- E-mail your question via the Internet to help@sti.nasa.gov
- Fax your question to the NASA Access Help Desk at 301-621-0134
- Telephone the NASA Access Help Desk at 301-621-0390
- Write to:
NASA Access Help Desk
NASA Center for AeroSpace Information
7121 Standard Drive
Hanover, MD 21076



The High Power Electric Propulsion (HiPEP) Ion Thruster

John E. Foster, Tom Haag, and Michael Patterson
Glenn Research Center, Cleveland, Ohio

George J. Williams, Jr.
Ohio Aerospace Institute, Brook Park, Ohio

James S. Sovey
Alpha-Port, Inc., Cleveland, Ohio

Christian Carpenter
QSS Group, Inc., Cleveland, Ohio

Hani Kamhawi, Shane Malone, and Fred Elliot
Glenn Research Center, Cleveland, Ohio

Prepared for the
40th Joint Propulsion Conference and Exhibit
cosponsored by the AIAA, ASME, SAE, and ASEE
Fort Lauderdale, Florida, July 11-14, 2004

National Aeronautics and
Space Administration

Glenn Research Center

Acknowledgments

The authors would like to acknowledge the technical assistance and dedication of Robert Roman, John Miller, Luis Pinero, George Soulas, and Don Fong to this project. The authors also thank Thomas Doehne for the layout and generation of thruster design drawings. Their tireless efforts on thruster fabrication and power console optimization contributed greatly to flow of the project.

Available from

NASA Center for Aerospace Information
7121 Standard Drive
Hanover, MD 21076

National Technical Information Service
5285 Port Royal Road
Springfield, VA 22100

Available electronically at <http://gltrs.grc.nasa.gov>

The High Power Electric Propulsion (HiPEP) Ion Thruster

John E. Foster, Tom Haag, and Michael Patterson
National Aeronautics and Space Administration
Glenn Research Center
Cleveland, Ohio 44135

George J. Williams, Jr.
Ohio Aerospace Institute
Brook Park, Ohio 44142

James S. Sovey
Alpha-Port, Inc.
Cleveland, Ohio 44135

Christian Carpenter
QSS, Inc.
Cleveland, Ohio 44135

Hani Kamhawi, Shane Malone, and Fred Elliot
National Aeronautics and Space Administration
Glenn Research Center
Cleveland, Ohio 44135

Practical implementation of the proposed Jupiter Icy Moon Orbiter (JIMO) mission, which would require a total delta V of approximately 38 km/s, will require the development of a high power, high specific impulse propulsion system. Initial analyses show that high power gridded ion thrusters could satisfy JIMO mission requirements. A NASA GRC-led team is developing a large area, high specific impulse, nominally 25 kW ion thruster to satisfy both the performance and the lifetime requirements for this proposed mission. The design philosophy and development status as well as a thruster performance assessment are presented.

I. Introduction

High power nuclear electric propulsion (NEP) systems are an enabling technology that has the potential to allow for the intensive exploration of the outer planets. Additionally, ample power for mission science and communications would be available via the nuclear power source. This on-board power source eliminates the solar flux penalty that limits the practical reach of solar electric propulsion to the inner solar system. The ample power of a NEP system would allow for continuous thrusting over the period of the expected life of the reactor, which for liquid metal cooled systems such as the SP-100 ranges between 7 and 10 years.¹

The present state of the art in high efficiency, high specific impulse, electric propulsion systems is embodied in the NASA's Solar Electric Propulsion Application Readiness (NSTAR) ion thruster. This thruster operated for over 16,000 hours in space and over 30,000 hours during an extended life test (ELT).² While significant in its own regard, the use of NSTAR technology, is insufficient to satisfy life and performance requirements for long duration missions to the outer planets. Depending on the mission, required high specific impulse engine thrusting times can be a significant fraction of the lifetime of the reactor. For example, the proposed Jupiter Icy Moon Orbiter mission has a delta-V requirement of at least 38 km/s. Ion thruster systems used for such an application will be required to operate continuously for perhaps as long as 7-14 years.³⁻⁵ Such long continuous operation times place stringent lifetime requirements on thruster components and subsystems.

In an effort to develop the engine technology capable of satisfying the demanding performance and lifetime requirements for NEP class mission, a NASA Research Announcement (NRA) was issued. The NRA called for the development of a long life, high power, high specific impulse propulsion system that could satisfy requirements for nuclear-electric propulsion missions to the outer planets and beyond. The initial requirements as defined by the NRA are listed below:

- Specific impulse = 6000 to 9000 seconds
 - Thruster Efficiency >65%
- NEP system specific mass = 30 kg/kW
 - Propellant throughput = 100 kg/kW

Thruster requirements have since changed becoming more stringent with power, specific impulse, and throughput/life so as to satisfy Jupiter Icy Moon Orbiter (JIMO) mission requirements.⁴ This translates into very long thrusting times (7-14 yrs) depending of specific impulse.

The research announcement has led to the development of two gridded ion thruster systems. The High Power Electric Propulsion (HiPEP) project led by NASA Glenn Research Center (GRC) and the Nuclear Electric Xenon Ion Thruster System (NEXIS) project led by NASA's Jet Propulsion Laboratory (JPL) responded to NASA's research announcement to develop such a propulsion system. The NEXIS thruster system approach was to leverage the heritage embodied in the NSTAR and the NASA Evolutionary Xenon Ion Thruster (NEXT) thruster.^{6,7} The HiPEP approach infuses technologies such as a rectangular discharge chamber, long life grid materials, and flexible discharge plasma production (DC or microwave electron cyclotron resonance). This approach addresses the primary thruster failure modes. The development of these technologies was seen as necessary since the life requirements will require significant hurdles over the state of the art. As such, the development of these technologies is focused on mitigating both cost and schedule risk.

The focus of this report is to give a general description of the HiPEP thruster, addressing the philosophy of the approach, the implementation, and analysis of data to date characterizing engine operation. Details regarding HiPEP project structure and overall scope may be found in the companion reference.⁸

Based on findings from mission analysis for 8000 s specific impulse, a 25 kW design point was chosen as the baseline operation point. In order to respond to potential changes in the JIMO specific impulse requirement, a 6000 s specific impulse, 25 kW was selected as a secondary design point.

II. Design Considerations

In general, thruster lifetime is limited by essentially five potential failure modes: 1.) discharge cathode failure, 2.) neutralizer cathode failure, 3.) electron backstreaming, 4.) erosion induced structural failure of the ion extraction grids, and 5) formation of an uncleanable short between grids. The failure mechanism of the cathode assembly is multi-faceted in that subcomponents such as heater failure and keeper assembly erosion can ultimately lead to component failure. Cathode failure modes can be loosely grouped into two general areas: physical erosion via sputtering and emitter element depletion of low work function material. Physical sputter erosion of the cathode assembly occurs because the cathode is constantly subjected to ion bombardment from the surrounding discharge plasma. Emitter failure is related to thermo-chemical processes that render the cathode incapable of supplying electrons even if other conditions such as thermal environment and pressure are adequate. Provided gas cleanliness protocols are followed (eliminates emitter poisoning), emitter failure occurs after long operation times because of the depletion of work function lowering impregnates at the emission sites. Additionally, the high temperature formation of inert or emitter pore-plugging compounds also effectively reduce the supply of work function lowering impregnates. Conventional ion thruster hollow cathodes have a demonstrated lifetimes of order 28,000-30,000^{2,9} hours. Longer hollow cathode lifetimes need to be demonstrated for these components to be compatible with those missions requiring continuous thruster operation in excess of that demonstrated to date. Failure mode 3 is related to electron backstreaming which occurs when accelerator grid apertures widen (at fixed accelerator grid voltage) due to erosion. When the aperture is sufficiently large, the positive potential associated with the screen grid can "leak" downstream of the ion optics assembly. When this occurs, electrons from the beam plasma can actually backstream into the engine achieving energies approximately equal to the beam voltage. This energetic beam of electrons can quickly overheat or damage the discharge cathode. Failure mode 4 is associated with severe grid erosion. Sputter erosion of the ion extraction grids can ultimately lead to thruster failure. Erosion of these components occurs primarily by charge exchange erosion. If the beamlets are not well focused, erosion due to direct impingement can also occur. Over time, these ion milling processes lead to structural degradation of the ion optics assembly, leading to poorer discharge performance over time and ultimately the cantilevering of one electrode into the other, giving

rise to a short and thereby terminating beam extraction. One potential solution to this problem is the use of a magnetic grid.¹⁰ Potential design solutions also exist for increasing the lifetime of the ion optics by using different electrode materials such as titanium¹¹ or carbon¹²⁻¹³ or by simply increasing the electrode thickness.¹⁴ Failure mode 5 involves unclearable shorts between the grids. The formation of large conducting flakes formed either from the erosion of the ion optics electrodes or by erosion of the discharge cathode assembly also can lead to ion optics failure. If the conducting flake were to bridge the gap between the high voltage ion optics grids, the resulting short would also terminate beam extraction. Another grid shorting mechanism is caused by unattached debris from spacecraft surfaces shorting the grids. This event has the highest probability of occurring during the launch phase.

As mentioned, the primary failure modes of the thruster are associated failure of the discharge cathode and the ion optics. As lifetime is the key parameter, the HiPEP approach necessarily focuses on greatly exceeding the state of the art for the various ion thruster component technologies. The HiPEP thruster design and development effort focuses on the elimination of failure modes.

A. Plasma Production

The HiPEP project approaches the main discharge plasma production issue with a two prong approach: DC hollow cathode and microwave electron cyclotron resonance (ECR) plasma generation. Both DC and microwave approaches have been developed. The DC plasma generator is the HiPEP thruster baseline approach. The DC approach utilizes a NEXT-like discharge cathode.¹³ Discharge current requirements for the 8000 s specific impulse design point are consistent with the operating range of the NEXT thruster discharge cathode assembly. This discharge cathode emitter is significantly larger than the NSTAR emitter insert. The larger emitter increases device lifetime by virtue of the fact that the impregnate reservoir is larger. The larger insert and orifice size accommodate higher emission current densities than the NSTAR design, with emission currents in excess of 40 A. This emission current range provides significant margin at the 8000 s specific impulse operating point. The discharge cathode keeper, which serves as a cathode physical shield against sputtering ions, is subject to erosion and can give rise to potential failure mechanisms such as formation of large, conducting flakes. Complete erosion of the keeper face plate, as was observed in the NSTAR 30,000 hr extended life test.² In order to minimize cathode assembly erosion due to physical sputtering, the main discharge cathode will utilize a graphite keeper. Because the sputter threshold of xenon ions on graphite is greater than the energies of the expected ion flux (discharge voltage~25 V), the use of the graphite keeper should eliminate this failure mechanism.¹⁵

The backup plasma generation approach involves the complete replacement of the hollow cathode assembly with an electrodeless plasma production. Microwave ECR has been investigated under the HiPEP project as an approach to eliminate the potential discharge cathode failure mechanisms. This technology has been demonstrated as a viable plasma production option.¹⁶⁻²⁰ Indeed, ECR ion thruster technology has been used as the primary propulsion for the MUSES-C asteroid rendezvous mission.¹⁹⁻²⁰ This electrodeless plasma production approach, depicted in Fig. 1 utilizes microwaves that heat electrons resonantly in the presence of a magnetic field. At this resonance, the electrons can gain energy continuously. This resonant process takes place on surfaces of constant magnetic field that are established by the magnetic circuit. The hot electrons produced during this process ionize neutral gas, thereby generating the discharge plasma completely electrodelessly. The process takes place away from discharge chamber walls, thereby minimizing wall erosion. Plasma potentials associated with ECR plasmas are typically significantly less than conventional hollow cathode devices.¹⁶ In this regard, the sputtering of the upstream surface of the screen grid can be virtually eliminated as the ions will strike the grid at energies associated with the Bohm speed.

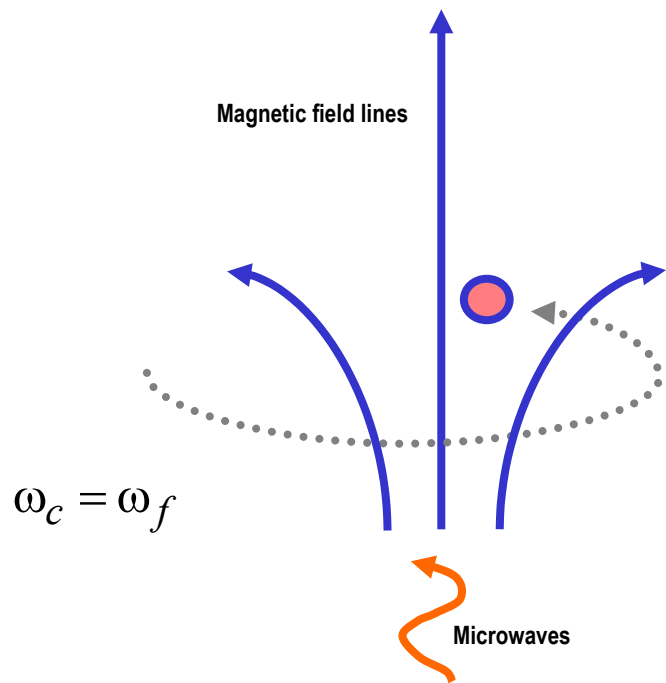


Figure 1. Conceptual depiction of electron cyclotron resonance heating. Resonance occurs when the microwave frequency ω_f is equal to the electron cyclotron frequency, ω_c .

The implementation of the microwave ECR approach for HiPEP employs the use of a slotted antenna. The slotted antenna affords the opportunity for distributed plasma production. Distributed plasma production yields uniform plasma density profiles at the optics exit plane, resulting in very flat beam profiles. Recall flat beam profiles are desirable in that they circumvent issues such as a reduced perveance limit and accelerated, localized accelerator grid wear on centerline. The microwave energy source proposed by HiPEP for the thruster application is a klystron. It is expected that the klystron should have lifetimes of order that of space qualified tubes such as the traveling wave tube (TWT). TWTs have demonstrated on-orbit lifetimes in excess of 144 kHrs.²¹⁻²³

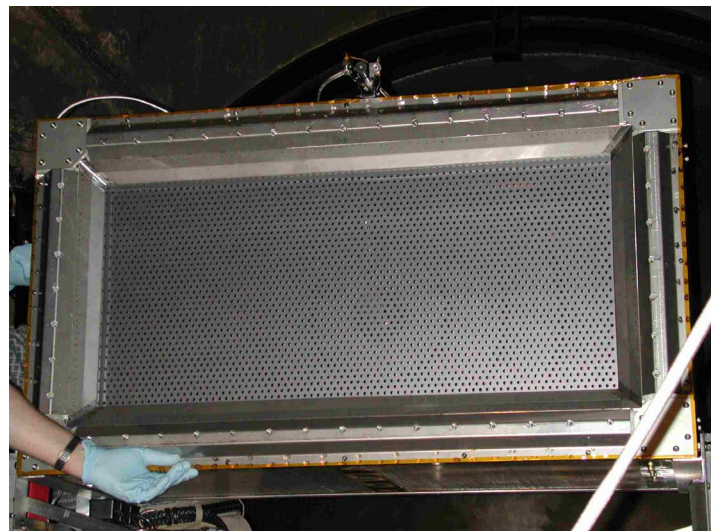
The HiPEP main discharge chamber is rectangular in geometry and is designed to accommodate either the baseline hollow cathode plasma production approach or microwave plasma production. The target plasma production efficiency for the HiPEP engine < 200 W/A while the design discharge chamber propellant utilization target is > 90%. Both plasma production approaches have been demonstrated with the rectangular discharge chamber. The thruster, shown in Fig. 2(a), is large, with an ion extraction exit plane measuring 41 x 91 cm. The large ion extraction area allows the thruster discharge chamber to operate at a lower current density than contemporary thrusters. Reduced beam current density reduces grid wear rates.

To achieve the target discharge chamber efficiency and propellant utilization goals, magnetic field calculation software was used to guide in the design and optimization of the ring cusp magnetic field geometry chosen. Ring cusp magnetic circuit electron containment schemes have been shown to be very efficient.²⁴ In the case of the HiPEP thruster, the shape of the magnetic rings range from circular to hybrid circular-rectangular to rectangular. Such ring geometries are necessary to accommodate the discharge chamber shape. The discharge chamber itself is made of non-ferrous steel. High field strength, rare earth magnets comprise the magnetic circuit. The magnetic circuit design accommodates the large volume plasma production necessary for thruster operation at the design points. Regions of low magnetic field strength, away from the walls, comprise a significant fraction of the internal discharge chamber volume. The termination plane of the discharge chamber is relatively field free and thus offers ease of flow of plasma ions to the ion extraction grids.

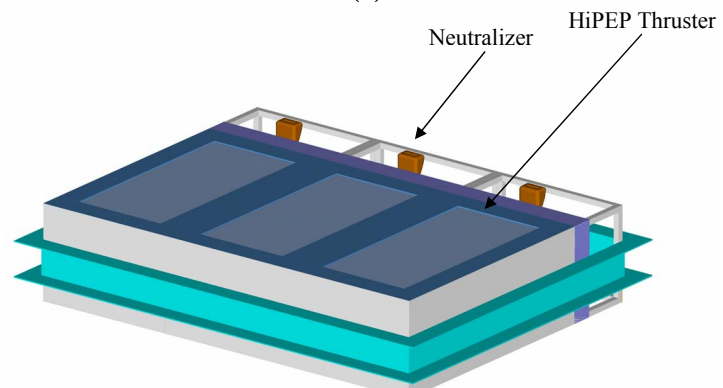
B. Discharge Chamber Shape, an Aside

It should be pointed out that the rectangular shape of the discharge chamber and associated plasma screen is well shaped for multiple thruster installations. Many thrusters can be installed adjacent to each other, forming a dense cluster of aligned ion beams. For multi-megawatt spacecraft, close packing may be desirable in order to consolidate structural mass, and minimize spacecraft appendages. Close packing may also enable collective beam neutralization, either with redundant neutralizers, or a few high capacity plasma contactors. Thermal management issues associated with close packing of engines can be addressed by simply mounting the thrusters in a manner such that the back-plate of the engines is exposed to the vacuum of space, thereby allowing the engines to freely radiate out of this plane. Fig. 2(b) depicts an artist conception of a possible HiPEP packing approach for rectangular geometry ion engines.

From a power processing standpoint, a primary attribute of the rectangular geometry



(a)



(b)

Figure 2. (a) HiPEP rectangular thruster featuring large area ion optics. (b) Conceptual depiction of HiPEP thruster pod: Rectangular thruster geometry is particularly amenable to “pack and stack” integration.

is scalability. The ability of the thruster discharge chamber to grow in size to accommodate higher power operation is an important thruster attribute in that it provides the flexibility to accommodate changes as mission requirements vary. Such flexibility also allows the engine to be applicable to a range of missions requiring different power levels. The rectangular geometry can accommodate significant increases in cross sectional area by simply increasing its lateral dimension. Because the internal magnetic circuit is rectangular in geometry as well, all that is required of the magnetic circuit to be consistent with increasing of the lateral dimension is simple lateral “stretching.” In this respect the local magnetic field environment away from the ends of the rectangular ring does not change. In other words, the discharge plasma experiences virtually the same magnetic environment as its smaller area counterpart. This insensitivity of the magnetic environment to lateral growth (particularly in the case of the microwave plasma production approach) is in sharp contrast with cylindrical devices where the curvature of each magnet ring and thus the local magnetic field changes appreciably with changes in diameter. In this regard, magnetic circuit re-design is necessary to assure comparable performance in cylindrical devices as it is scaled up in diameter.

C. Ion Extraction Electrodes

Like the discharge chamber, the ion optics electrodes are also of rectangular geometry. The 2-grid ion extraction system is manufactured from flat, pyrolytic graphite sheet. The pyrolytic graphite sheet has a significantly lower sputter yield at relevant energies than molybdenum, which is used for the NSTAR and NEXT thrusters. For example, the sputter yield of xenon ions on carbon is 1/5 that of xenon on molybdenum at 500 eV. Additionally, the grids are large in cross-sectional area—over 5 times that of the NSTAR thruster. The large grid extraction surface area allows reduction in beam current density, which in turn contributes to reduced charge exchange erosion rates. To increase the beam extraction area of a conventional circular thruster, the ion optics diameter must increase. The grid span to gap ratio increases proportionally, resulting in a more challenging mechanical design. With grid gap controlled by electrical standoffs located only around the perimeter, the mid-span region may be subject to significant gap variability. Deformation due to electrostatic attraction, thermal strain, and launch vibration become worse as the unsupported span increases in length. This is unfortunate since typically for hollow cathode driven ion thruster discharges, the center region often has the highest beam current density and thus highest thermal load. With a rectangular ion optics geometry, the maximum length of unsupported span is bounded by the rectangle width. Ion beam extraction area can be increased significantly by increasing thruster length, but the grid gap remains closely controlled across its width.

The aforementioned ion optics attributes give the HiPEP thruster significant life margin. Indeed, the baseline grid geometry accommodates a 100 kg/kW throughput with margin at both the 8000 s and 6000 s specific impulse design points. Further details regarding ion optics performance may be found in reference 25.

D. The Neutralizer

The HiPEP neutralizer must satisfy a number of stringent requirements:

1. Provide up to 6-9 A of electron emission current necessary for beam neutralization.
 - a. Demonstrate growth potential electron emission currents in excess of 9 A.
 - b. The neutralizer must be capable of supplying 6-9 A continuously for periods 7-14 years
 - c. Erosion processes must be well understood and appropriately addressed by both model and extended wear tests.
 - d. Electron extraction voltages must be sufficiently low (ideally less than threshold sputter energy).
 - e. Multiply-charged ion fractions must be minimized to reduce the erosion of neutralizer surfaces.
 - f. Electron emitting temperature and chemistry must be well understood to ensure there will be no migration of materials to the vicinity of the cathode orifice.
2. The neutralizer design must attempt to minimize mass, volume and gas flow requirements with the NEXT neutralizer as a baseline reference.
 - a. HiPEP thruster design points are optimized such that flow allotment for the neutralizer at 3.5 A beam is approximately 5 sccm and 7 sccm at 6 A beam current. Neutralizer flow rate optimization impacts total propellant efficiency, specific impulse, and total thruster efficiency. (A beam current of about 3.5 A is required for operation at 25 kW and 8000 s specific impulse.)

Two different neutralizer approaches are being investigated under the HiPEP project. The baseline approach utilizes a conventional hollow cathode. This baseline approach was selected because conventional hollow cathode-based neutralizers are 1) capable of supplying the required electron flux at acceptable expenditure of power and xenon flow, and 2) the neutralizer assembly undergoes reduced erosion relative to the discharge cathode.²⁶ This

latter point is bolstered by observed state of the ELT NSTAR thruster neutralizer determined after termination of the wear test.²⁶ After over 30,000 hours of testing, with the exception of the underside of the keeper tube that faces the beam, the neutralizer's condition was fairly pristine. Indeed, the neutralizer continued to operate nominally over the duration of the wear test. The reason for the apparent immunity to degradation resides in the fact that the neutralizer is not immersed in a dense plasma. Additionally, the potential of the neutralizer and the local space potential is typically less than the sputter threshold for neutralizer materials.

The presence of the keeper tube underside erosion determined post ELT suggests direct impingement or enhanced charge exchange erosion. Fabrication of the keeper from graphite would address enhanced charge exchange erosion occurring between the beam plasma and the neutralizer plasma. It, however, does not address potential erosion driven by extreme off-axis beam ions. This issue can be practically addressed by optimizing the neutralizer's position. Such an optimization study is necessary in order to avoid off-axis direct impingement, which over test durations much longer than the NSTAR ELT could be a potential life limiter.

The above-mentioned issues address erosion issues associated with physical sputtering. In addition to physical sputtering, the neutralizer lifetime is also a function of emitter condition. Barium depletion for all practical purposes represents emitter end-of-life. Provided the physical sputtering issue is solved via position optimization and the integration of a graphite keeper, two approaches are considered to extend neutralizer system life. First, design criteria, life models, and supporting neutralizer test data will be obtained to validate the lifetime of conventional hollow cathodes meeting or exceeding JIMO requirements. Secondly, multiple neutralizers may be employed. The number of neutralizers required is determined by the defined life per neutralizer. The product of the life per neutralizer and the total number of neutralizers can be optimized such that it exceeds the mission lifetime requirement by approximately 1.5 (for margin.)

A microwave neutralizer is also being developed under the HiPEP activity. The basis of this activity is primarily risk mitigation. Microwave neutralizers have been used successfully for at least one deep space mission—MUSES C.²⁷⁻²⁸ In the strictest sense, the microwave neutralizer is essentially a plasma cathode. This concept is illustrated in Fig. 3. Electrons are extracted from the boundary of a very dense discharge plasma.²⁹ Extracted electrons can also generate additional electrons via collisions with gas exiting the neutralizer. This plasma bridge reduces impedance and thereby reduces the neutralizer extraction voltage. Integration of a microwave neutralizer with a microwave main discharge plasma generator in addition to providing extended life, also simplifies power supply and feed system requirements and eliminates gas cleanliness protocols. Both internal antenna and slotted antenna approaches are viable options for neutralizer plasma generation that have been actively pursued under the HiPEP project.³⁰

III. Thruster Evolution

From a manufacturing standpoint, the rectangular prism shape of the discharge chamber and the planar rectangular grid electrodes make fabrication fairly straightforward. Indeed, involved manufacturing processes such as spin-forming, typical of cylindrical geometries and ion optics dishing, are not required. The discharge chamber itself is consists of flat stainless steel panels to which flake containment mesh is attached. Assembly of the panels using angle bracket or the like is relatively straightforward. Magnets are mounted on the outside of the rectangular discharge chamber. The magnets are attached to the outer shell via stainless steel channel retainers. Mounting the magnets on the outside reduces the heat load to an individual magnet ring. Integration of the plasma generation approach, be it hollow cathode or microwave, is also straightforward.

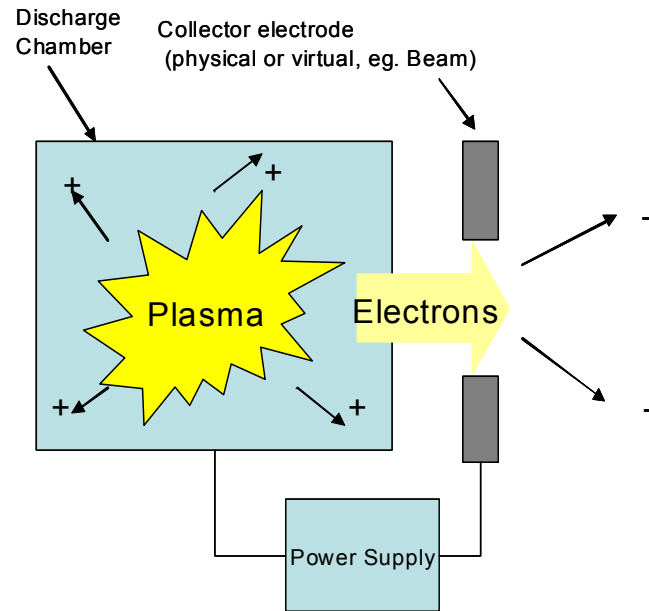


Figure 3. Generalization of a plasma cathode electron source. Electron current is extracted from a dense plasma formed within the discharge cavity. Cavity plasma is generated via ECR .

The test objectives of the laboratory version of the HiPEP thruster are to map out performance and provide insight into optimization. These goals include: 1) optimize discharge performance (discharge losses, propellant utilization, and plasma uniformity (beam flatness), 2) optimize grid performance (perveance margin and backstreaming limit), and 3) evaluate neutralizer performance.

Based on results of this optimization process the overall engine design will evolve by incorporating performance improving changes to the geometry and magnetic circuit. Early on, a first generation laboratory model was fabricated and tested. Lessons learned from this model were used to fabricate a second generation laboratory model. The development model that will be wear-tested incorporates performance improving changes ascertained in the second generation laboratory model. This process of building on successive generations of thrusters improves overall design and reliability by incorporating lessons learned and establishing heritage. Thermal and structural optimization is also incorporated during the design evolution process. These modifications are guided by actual test data and modeling such that the end product of is a high fidelity, development model thruster.

IV. Thruster Wear Test

A preliminary assessment of the thruster's performance over time is planned for the HiPEP thruster. The duration of the test will be 2000 hrs. In addition to assessing the thruster's performance over time, another function of the test will be to determine any previously unknown failure modes. Though the wear test duration is considerably short relative to the required lifetime of the thruster system (~10 years), some insight regarding lifetime is expected to be gleaned from the test. For example the issue of flake containment, neutralizer keeper and discharge cathode keeper erosion, and unexpected grid erosion can be assessed from such a test. Findings from the wear test will be utilized in the JPL-led JIMO thruster life evaluation task.

For wear test results to be meaningful, the wear test facility has to have sufficient pumping speed as well as sufficiently low backsputter rate. Poor background pressure enhances charge exchange erosion and affects thruster performance and wear. High backsputter rates give rise to deposition that could mask any erosion accumulated over the 2000 hrs. Vacuum facility 6 at NASA GRC will be the HiPEP wear test cell. The tank measures 7.6 m by 21m with a pumping speed of approximately 300 kl/s on xenon.³¹ Expected backsputter rates at the 25 kW, 8000 s specific impulse operating point should be of order 1-2 micron/kh. Baseline diagnostics to be utilized in the wear test include cameras, beam probes and deposition sensors (quartz crystal microbalance, witness plates, pinhole cameras).

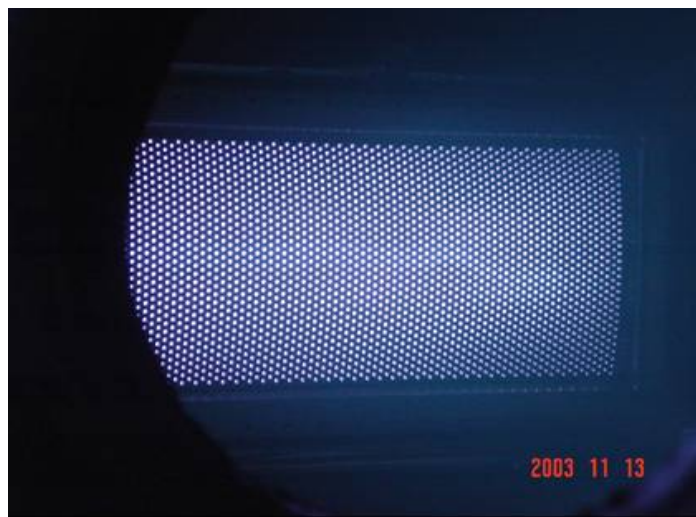
V. Thruster Performance and Development Status

To date the HiPEP thruster has been operated using two plasma generation approaches. The DC plasma generation approach was selected as the primary plasma generation approach because it offered the lowest risk to schedule. The primary objective of the backup microwave effort was to have a fully developed, high performance microwave plasma generator available if in the event, life limitations or implementation issues associated with hollow cathode technology enhances risk to the project. The first HiPEP engine beam extraction test was conducted at beam powers up to 16 kW using 2.45 GHz microwaves. The design microwave frequency for the HiPEP engine is actually 5.85 GHz. In the early test, 2.45 GHz was used because it was available and provided a low risk demonstration of the concept. The higher frequency operating design point significantly increases the plasma density and thus propellant utilization as well as maximum extractable beam current. Specific impulse for 2.45 GHz test ranged between 4500s to 5500s. The test illustrated that large volume, uniform plasma could be generated using microwave ECR. Figure 4 illustrates microwave thruster in operation along with an ion beam profile. Beam flatness (the ratio of average to peak current density) of over 0.82 was measured with microwave ECR, demonstrating the ability to produce uniform plasma profiles at the ion extraction plane. The test represented the largest (size and power) ECR ion source ever operated. Subsequent microwave engine testing was done at 5.85 GHz, the thruster design frequency. These higher frequency tests were aimed at discharge performance optimization. Microwave thruster discharge testing at 5.85 GHz demonstrated the higher plasma production capacity as compared to 2.45 GHz. At this higher frequency, simulated ion grid currents over 4 A were measured, well above that which is needed for the 8000 s design point.

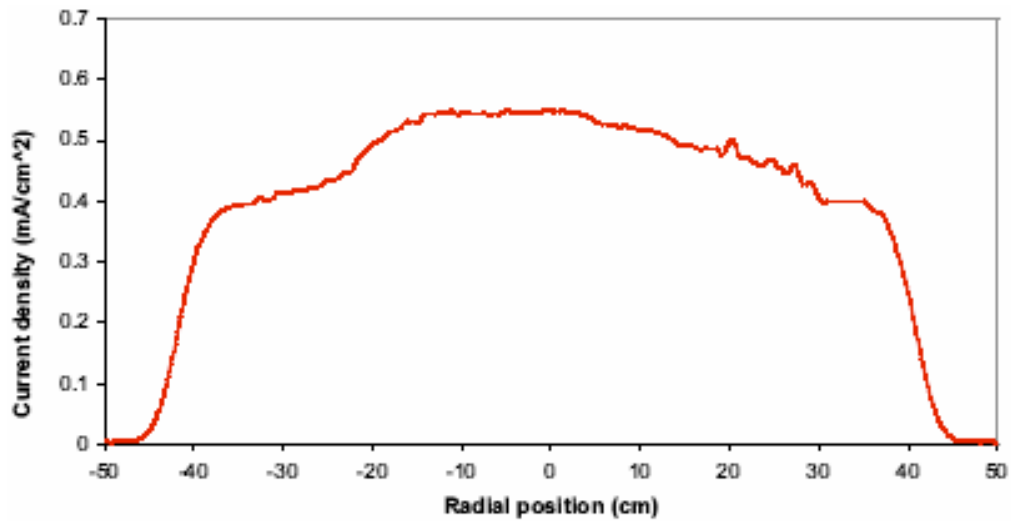
The DC HiPEP engine has been performance characterized at power levels up to 40 kW. A photograph of the engine operating at 34 kW is shown in Fig. 5. Table I presents typical thruster performance over a power range between 10 and 40 kW. The data shown in the table has been corrected for ingested flow. The nominal specific impulse is approximately 8000 s, the primary design point. As can be seen here, there thruster performs well over a specific impulse range between 6000 and 10000 s. Total thruster efficiencies in excess of 75% were achievable at the higher power levels as indicated in the table.

Table I. DC HiPEP Thruster Performance

<i>Power, kW</i>	<i>Flow Rate, mg/s</i>	<i>Efficiency</i>	<i>Thrust, mN</i>	<i>Specific Impulse</i>
9.7	4.0	0.72	240	5970
15.9	4.9	0.74	340	7020
20.2	5.6	0.75	410	7500
24.4	5.6	0.76	460	8270
29.6	6.2	0.80	540	8900
34.6	6.6	0.77	600	9150
39.3	7.0	0.80	670	9620



(a)



(b)

Figure 4. Photograph of HiPEP engine operating with microwave ECR as the plasma production approach. (b) Beam profile at a beam current of 1.64 A.

Discharge chamber performance was assessed for the 8000 s specific impulse design point by plotting the discharge losses versus the discharge propellant utilization efficiency as shown in Fig. 6. Here the beam current and discharge voltage were fixed as flow rates and discharge current are adjusted to vary the discharge propellant utilization efficiency. Discharge losses were plotted as a function of utilization efficiency for two different discharge voltages. The discharge voltage at a given internal discharge chamber pressure determines the nature of the electron energy distribution function. In this respect, the discharge voltage will affect ionization efficiency for a given input total flow. The doubly charged xenon fraction typically increases at high propellant utilizations and associated high discharge losses. It is desirable to operate in the knee of the utilization curve because it is here where the required discharge power expenditure for a given beam current is minimized. It was observed that beyond the knee, at the higher propellant utilization efficiencies (>0.85), discharge losses were lower at the higher discharge voltage. This is likely related to improved ionization efficiency at the higher discharge voltage. For example, at 28 V, the discharge losses for operation at propellant efficiencies of 0.90 and 0.92 are 188 and 196 W/A, respectively. This is to be contrasted with the 25 V data in which discharge losses were greater 200 W/A for propellant efficiencies greater than 0.90. Because discharge power is a small fraction of total thruster power, operating at the 28 V discharge does not significantly impact performance. An assessment of the fraction of doubly charge ions will be necessary to determine if erosion is an issue for operation at 28 V.

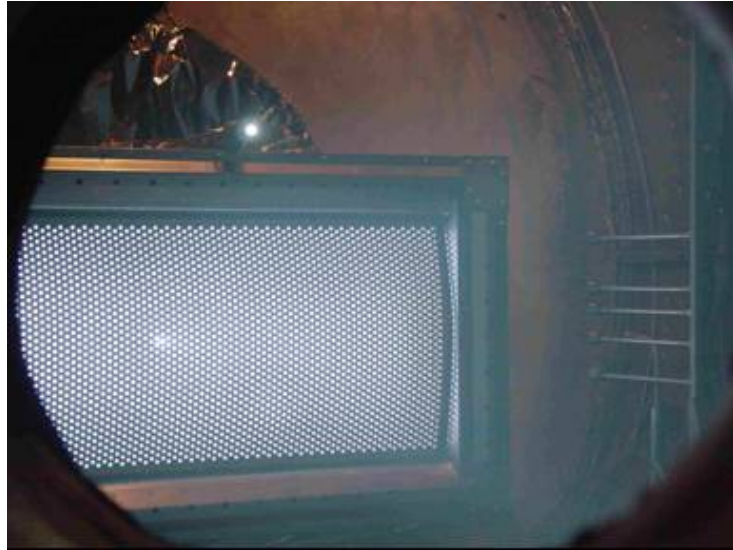


Figure 5. Photograph of the DC HiPEP engine operating at 34 kW.

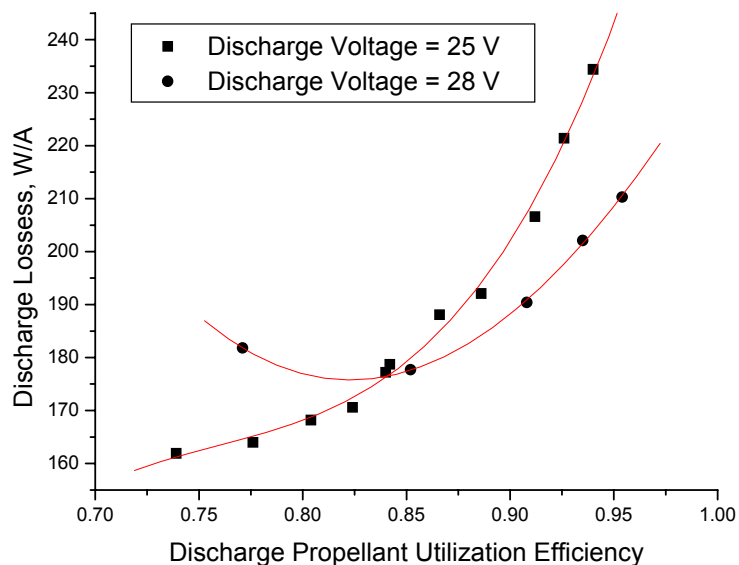


Figure 6. HiPEP engine discharge losses at the 8000 s design point.

Figure 7 illustrates the range and growth capacity for the ion thruster. Here thruster efficiency and specific impulse are plotted as a function of thruster power. For each curve, the propellant utilization efficiency and beam current were held fixed. The beam voltage was then varied to throttle in power. In general, under the conditions of fixed beam current and utilization, the specific impulse should increase as the square-root of the thruster power, provided the discharge power is a small fraction of the total input power (a situation which prevails here.) As can be seen here, the specific impulse increases as expected monotonically with increasing power (beam voltage). To verify the square-root dependence, a function of the form $y = a \cdot x^b$, where a and b are fitting parameters, was fit to each power throttling curve. The constant b should be approximately 0.5, indicating the expected square root relationship with power. For the data shown here, b was found to be approximately 0.53, which is in good agreement with the expected scaling.

Thruster efficiencies greater than 65 % (NRA requirement) were demonstrated even for power levels as low as 6 kW as indicated in Fig. 7. Here, the solid line indicates the NRA efficiency requirement. The thruster efficiency indicates a small positive slope as beam voltage (thruster power) is increased. Strictly speaking, if ion extraction efficiency does not vary, the thruster efficiency should be essentially flat or constant over the power range. The small deviation is most likely attributed to an increase in screen grid transparency which typically increases with increasing beam voltage.³² This increase results in a slightly reduced discharge power requirement for a given beam current, thereby resulting in an improvement in thruster efficiency with increasing thruster power. Power levels up to nearly 40 kW are also illustrated in Fig. 7. Power levels above 40 kW were limited only by power supply output capacity. In all cases, discharge propellant utilization efficiency was ~0.9 or better. Over this power range, specific impulse values of 7000 s to 9000 s were demonstrated. The family of curves in Fig. 7 illustrates the growth potential and overall range of the thruster.

Thrust as a function of input power at a nominal specific impulse centered at 8000 s is illustrated in Fig. 8. The beam voltage is essentially fixed for the data presented in the figure. Under these conditions, thrust should be a linear function of thruster input power. This functional relationship is illustrated in the figure. For all data points illustrated in the figure, the average thruster efficiency was greater than 75%.

Presently, a development model thruster is being prepared for wear testing. It will be nearly identical to the previous generation thruster used in performance tests with a few notable exceptions: 1) magnet rings will be attached to the outside of the discharge chamber 2) flake containment mesh will be installed on discharge chamber inner surfaces 3) ion optics mount system will be of higher fidelity from a structural standpoint, and 4) the discharge cathode will feature a graphite keeper electrode. The objective of the wear test will be to measure the thruster's capacity to operate reliably over extended duration, reveal yet unidentified failure mechanisms, and make a limited assessment on thruster life.

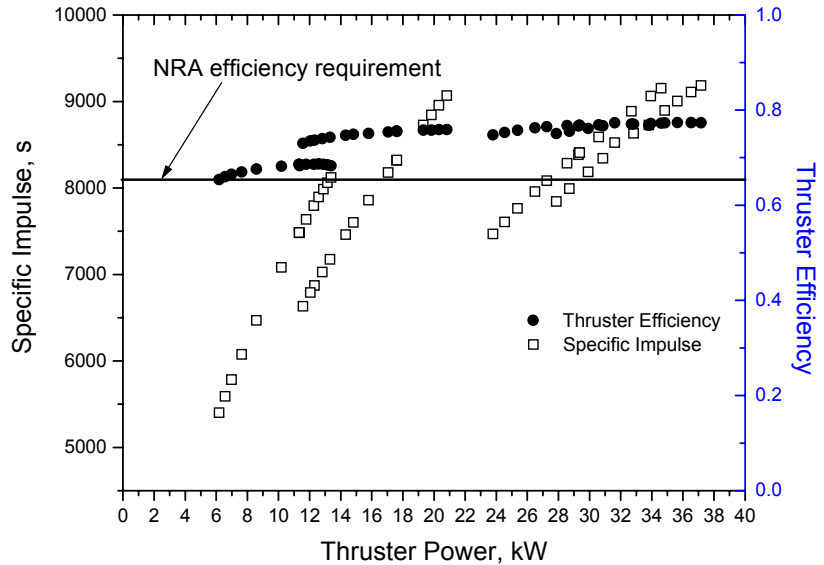


Figure 7. HiPEP engine power throttling range demonstrates high efficiency over a wide power range.

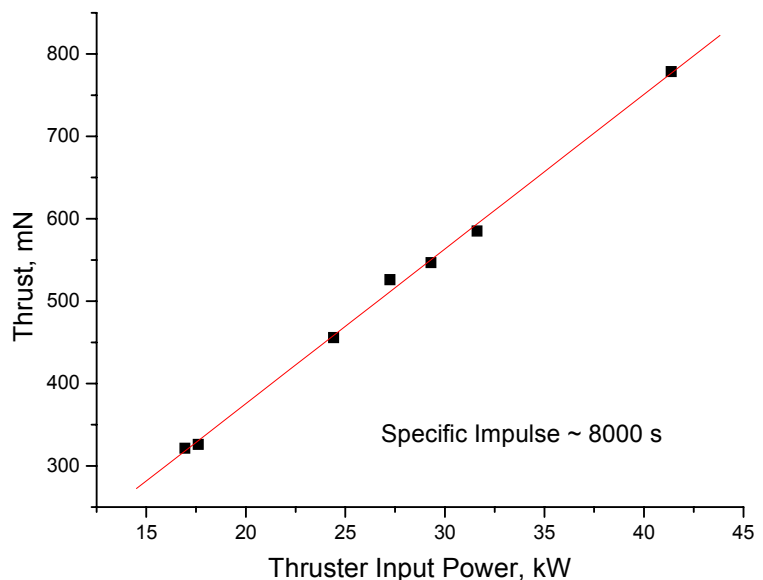


Figure 8. HiPEP thruster thrust variations as a function of thruster input power.

VI. Concluding Remarks

The HiPEP project was one of three research efforts selected to develop a high power electric propulsion system to satisfy thruster requirements for NEP missions, in particular the proposed JIMO mission. The HiPEP project selected a large area, rectangular thruster geometry to address the requirements of high power and long life. The HiPEP project thruster has been fabricated and tested. The engine's design includes the integration of technologies aimed at increasing life well above to the state of the art by a factor of 3. These technologies include rectangular, pyrolytic graphite grids, large area discharge chamber and a discharge cathode assembly with a graphite keeper electrode. Microwave ECR plasma generation technologies are also being developed to mitigate risk. Performance testing confirms thruster growth potential to power levels well beyond the targeted 25 kW operating point. Efficiencies in excess of 0.75 have been measured over a range of thruster powers (20-40 kW). Presently a HiPEP development model thruster is being prepared for a 2000 hour wear test. The objective of the wear test is to demonstrate reliable extended duration operation as well as provide insight into wear mechanisms.

References

- ¹El-Genk, M.S., ed., A Critical Review of Space Nuclear Propulsion: 1984-1993, AIP Press, NY, 1994, pp. 22-23.
- ²Sengupta, A., et al, "Status of the Extended Life Test of the Deep Space 1 Flight Spare Ion Engine after 30,000 hours of Operation," AIAA Paper 2003-4558, July 2003.
- ³Patterson, M.J., Roman, R.F., and Foster, J.E., "Ion Engine Development for Interstellar Precursor Missions," AIAA Paper 2000-3811, July 2000.
- ⁴Oleson, S., "Electric Propulsion Technology Development for the Jupiter Icy Moon Orbiter Project," AIAA Paper 2004-3449, July 2004.
- ⁵Rawlin, V.K., Williams, G.W., Pinero, L.R., and Roman, R. F., "Status of Ion Engine Development for High Power, High Specific Impulse Missions," IEPC Paper 2001-096, October 2001.
- ⁶Polk, J.E, et al, "An Overview of the NEXIS Program," AIAA Paper 2003-4713, July 2003.
- ⁷Patterson, M.J., Foster, J.E., Haag, T., Soulas, G.C., Pastel, M.R., and Roman, R.F., "NEXT: NASA's Evolutionary Xenon Thruster Development Status," AIAA Paper 2003-4862, July 2003.
- ⁸Foster, J.E. et al, "An Overview of the HiPEP Project," AIAA Paper 2004-3453, July 2004.
- ⁹Kovaleski, S.D., Patterson, M.J., Soulas, G.C., and Verhey, T.R., "A Review of Hollow Cathode Testing for the International Space Station Plasma Contactor," IEPC Paper 01-271, October 2000.
- ¹⁰Foster, J.E., Roman, R., Soulas, G.S., and Patterson, M.J., "Magnetic Grid for Electron Backstreaming Mitigation," IEPC Paper 01-221, October 2001.
- ¹¹Soulas, G.C., Foster, J.E., and Patterson, M.J., "Performance of Titanium Optics on a NASA 30 cm Ion Thruster," AIAA Paper 2000-3814, July 2000.
- ¹²Shotwell, R., "Carbon-Carbon Grid Development for Ion Propulsion Systems," IEPC Paper 2001-093, October 2001.
- ¹³Haag, T., Patterson, M.J., and Soulas, G.C., "Carbon-Based Ion Optics Development at NASA GRC," IEPC Paper 2001-094, October 2001.
- ¹⁴Soulas, G.C., "Improving Total Impulse Capability of the NSTAR Ion Thruster with Thick-Accelerator -Grid Ion Optics, IEPC Paper 01-081, October 2001.
- ¹⁵Yamamura, Y. and Tawara, H., "Energy Dependence of Ion-induced Sputtering Yields from Monatomic Solids at Normal Incidence," Atomic Data and Nuclear Data Tables, Vol. 62, 149-253, 1996.
- ¹⁶Foster, J.E. and Patterson, M.J., "Discharge Characterization of 40 cm-Microwave ECR Ion Source and Neutralizer," AIAA Paper 2002- 5012, July 2002.
- ¹⁷Divergilio, W.F., Goede, H., and Fosnight, V.V., "High Frequency Plasma Generators," NASA CR-167957, November 1981.
- ¹⁸Toki, H., Fujita, H., Nishiyama, K., Hitoshi, K., and Funaki, I., "Performance Test of Various Discharge Configurations for ECR Discharge Ion Thruster," IEPC Paper 01-107, October 2001.
- ¹⁹Kuninaka, H., Satori, S., Funaki, I., Shimizu, Y., and Toki, K., "Endurance Test of Microwave Discharge Ion Thruster System for Asteroid Sample Return Mission MUSES-C," IEPC Paper 92-137, December 1997.
- ²⁰Toki, K., et al., "Technological Readiness of Microwave Ion Engine System for MUSES-C Mission," IEPC 01-174, October 2001.
- ²¹Park, S.S. et al., "Reliability Analysis of Klystron-Modulator System," *Proceedings of the Second Asian Particle Accelerator Conference*, Beijing, China, 2001.
- ²²Hansen, J.W., "US TWTs from 1 to 100 GHz," *Microwave Journal*, 1989, Vol. 32, pp. 179-183.
- ²³Dieumegard, D. et al, "Life Test Performance of Thermionic Cathodes," *Applied Surface Science*, Vol. 111, February, 1997, pp. 84-89.
- ²⁴Sovey, J.S., "Improved Ion Containment using a Ring-Cusp Ion Thruster," *Journal of Spacecraft and Rockets*, Vol. 21, Sept.-Oct. 1984, pp. 488-495.
- ²⁵Williams, G.W. , Sovey, J., and Haag, T., "Performance Characterization of HiPEP Ion Optics," AIAA Paper 2004-3627, July 2004.

²⁶Sengupta, A., Brophy, J.R., Garner, C.E., and Anderson, J.A., “An Overview of the Results from the 30,000 Hour Life Test of the Deep Space One Flight Spare Ion Engine,” AIAA Paper 2004-3608, July 2004.

²⁷Toki, K, Kuninaka, H., Nishiyama, K., Shimizu, Y., and Funaki, I., “Technological Readiness of Microwave Ion Engine system for Muses-C mission,” IEPC 01-120, October 2001.

²⁸Satori, S, Kuninaka, H., Ohtaki, M, and Ishikawa, Y., “Operational Characteristics of Microwave Discharge Neutralizer,” IEPC Paper 97-05, December 1997.

²⁹Oaks, E. M., “ Physics and Techniques of Plasma Electron Sources,” *Plasma Sources Sci. Technol.*, Vol. 1, 1992, pp. 249-255.

³⁰Kamhawi, H., Foster, J., and Patterson, M.J., “Parametric investigation of an ECR cathode,” AIAA Paper 2004-3819, July 2004.

³¹“ElectricPropulsionLaboratory:Facility Capabilities,” http://facilities.grc.nasa.gov/epl/epl_caps.html.

³²Soulas, G.C., Domonkos, M.T., and Patterson, M.J., “Performance Evaluation of the NEXT Ion Engine,” AIAA Paper 2003-5278, July 2003.

REPORT DOCUMENTATION PAGE

Form Approved
OMB No. 0704-0188

Public reporting burden for this collection of information is estimated to average 1 hour per response, including the time for reviewing instructions, searching existing data sources, gathering and maintaining the data needed, and completing and reviewing the collection of information. Send comments regarding this burden estimate or any other aspect of this collection of information, including suggestions for reducing this burden, to Washington Headquarters Services, Directorate for Information Operations and Reports, 1215 Jefferson Davis Highway, Suite 1204, Arlington, VA 22202-4302, and to the Office of Management and Budget, Paperwork Reduction Project (0704-0188), Washington, DC 20503.

1. AGENCY USE ONLY (<i>Leave blank</i>)		2. REPORT DATE September 2004	3. REPORT TYPE AND DATES COVERED Technical Memorandum	
4. TITLE AND SUBTITLE The High Power Electric Propulsion (HiPEP) Ion Thruster			5. FUNDING NUMBERS WBS-22-982-10-02	
6. AUTHOR(S) John E. Foster, Tom Haag, Michael Patterson, George J. Williams, Jr., James S. Sovey, Christian Carpenter, Hani Kamhawi, Shane Malone, and Fred Elliot				
7. PERFORMING ORGANIZATION NAME(S) AND ADDRESS(ES) National Aeronautics and Space Administration John H. Glenn Research Center at Lewis Field Cleveland, Ohio 44135-3191			8. PERFORMING ORGANIZATION REPORT NUMBER E-14693	
9. SPONSORING/MONITORING AGENCY NAME(S) AND ADDRESS(ES) National Aeronautics and Space Administration Washington, DC 20546-0001			10. SPONSORING/MONITORING AGENCY REPORT NUMBER NASA TM-2004-213194 AIAA-2004-3812	
11. SUPPLEMENTARY NOTES Prepared for the 40th Joint Propulsion Conference and Exhibit cosponsored by the AIAA, ASME, SAE, and ASEE, Fort Lauderdale, Florida, July 11-14, 2004. John E. Foster, Tom Haag, Michael Patterson, Hani Kamhawi, Shane Malone, and Fred Elliot, NASA Glenn Research Center; George J. Williams, Jr., Ohio Aerospace Institute, Brook Park, Ohio 44142; James S. Sovey, Alpha-Port, Inc., Cleveland, Ohio 44135; and Christian Carpenter, QSS Group, Inc., Cleveland, Ohio 44135. Responsible person, John E. Foster, organization code 5430, 216-433-6131.				
12a. DISTRIBUTION/AVAILABILITY STATEMENT Unclassified - Unlimited Subject Category: 20 Available electronically at http://gltrs.grc.nasa.gov This publication is available from the NASA Center for AeroSpace Information, 301-621-0390.			12b. DISTRIBUTION CODE	
13. ABSTRACT (<i>Maximum 200 words</i>) Practical implementation of the proposed Jupiter Icy Moon Orbiter (JIMO) mission, which would require a total delta V of approximately 38 km/s, will require the development of a high power, high specific impulse propulsion system. Initial analyses show that high power gridded ion thrusters could satisfy JIMO mission requirements. A NASA GRC-led team is developing a large area, high specific impulse, nominally 25 kW ion thruster to satisfy both the performance and the lifetime requirements for this proposed mission. The design philosophy and development status as well as a thruster performance assessment are presented.				
14. SUBJECT TERMS Nuclear electric propulsion; Ion thruster; Electric propulsion; Specific impulse; Microwave plasma; Hollow cathode			15. NUMBER OF PAGES 18	
			16. PRICE CODE	
17. SECURITY CLASSIFICATION OF REPORT Unclassified	18. SECURITY CLASSIFICATION OF THIS PAGE Unclassified	19. SECURITY CLASSIFICATION OF ABSTRACT Unclassified	20. LIMITATION OF ABSTRACT	

